Electronic Supplementary Information

Anionic ligand installed pyrene-based MOF for the fluorescent detection of paraquat

Bo Zhao, Qi Yang, Jia-Si Wang, Feng-Yang Xie, Hong-Yi Yu, Yue Li,* Yu-Xin Ma,* and Wen-Juan Ruan*

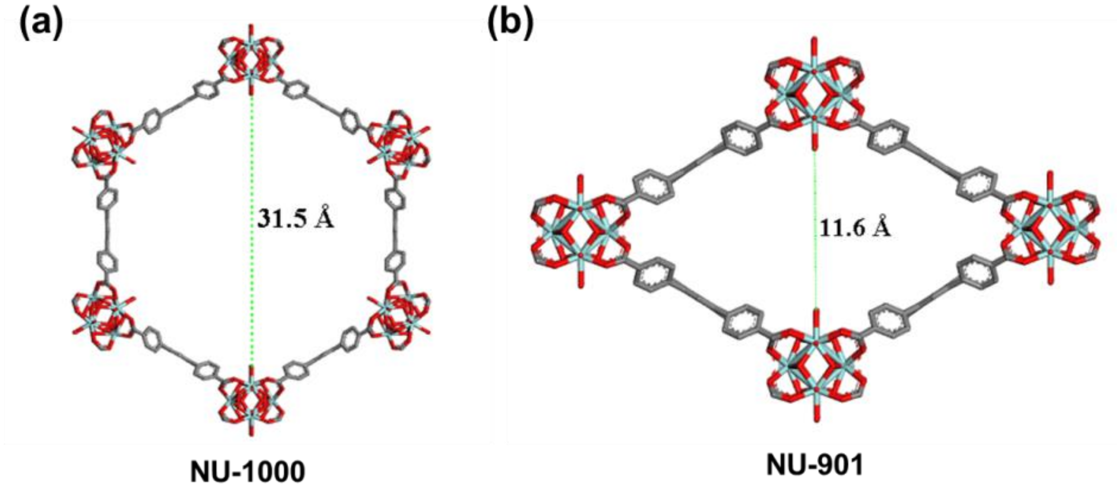

Fig. S1 Distances between the Zr_6 clusters on the ab plane of (a) NU-1000 and (b) NU-901.

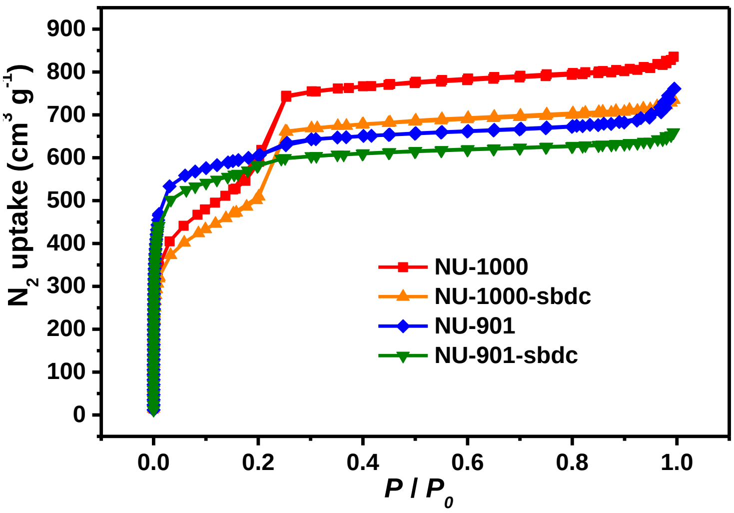

Fig. S2 N_2 adsorption isotherms (at 77 K) of activated NU-1000, NU-901 and their derivatives.

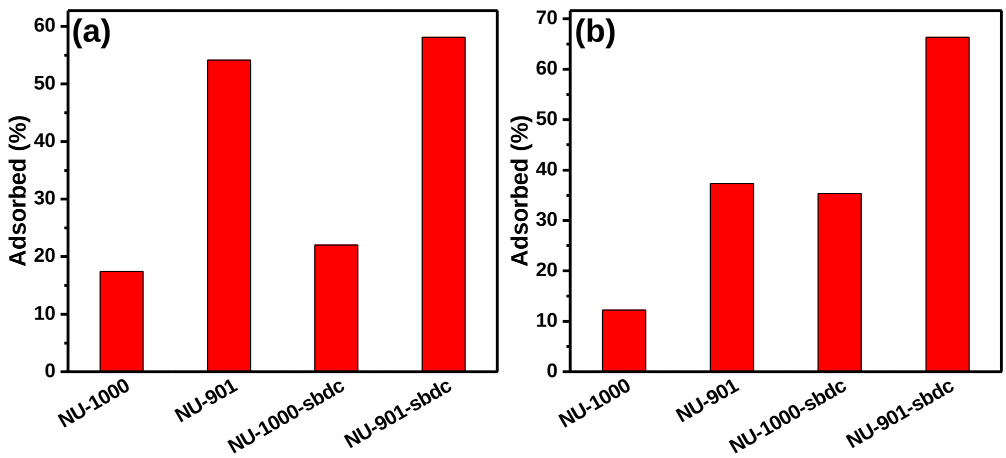

Fig. S3 Adsorbed percentages of paraquat (c_0 = 75 μM) by NU-1000, NU-901, NU-1000-sbdc and NU-901-sbdc (0.75 g L^{-1}) in (a) water and (b) DMF. Adsorbed percentages were calculated with the equation of adsorb.% = (A_{before} − A_{after}) / A_{before}, where A_{before} and A_{after} are the absorbances of paraquat solution before and after MOF adsorption, respectively.

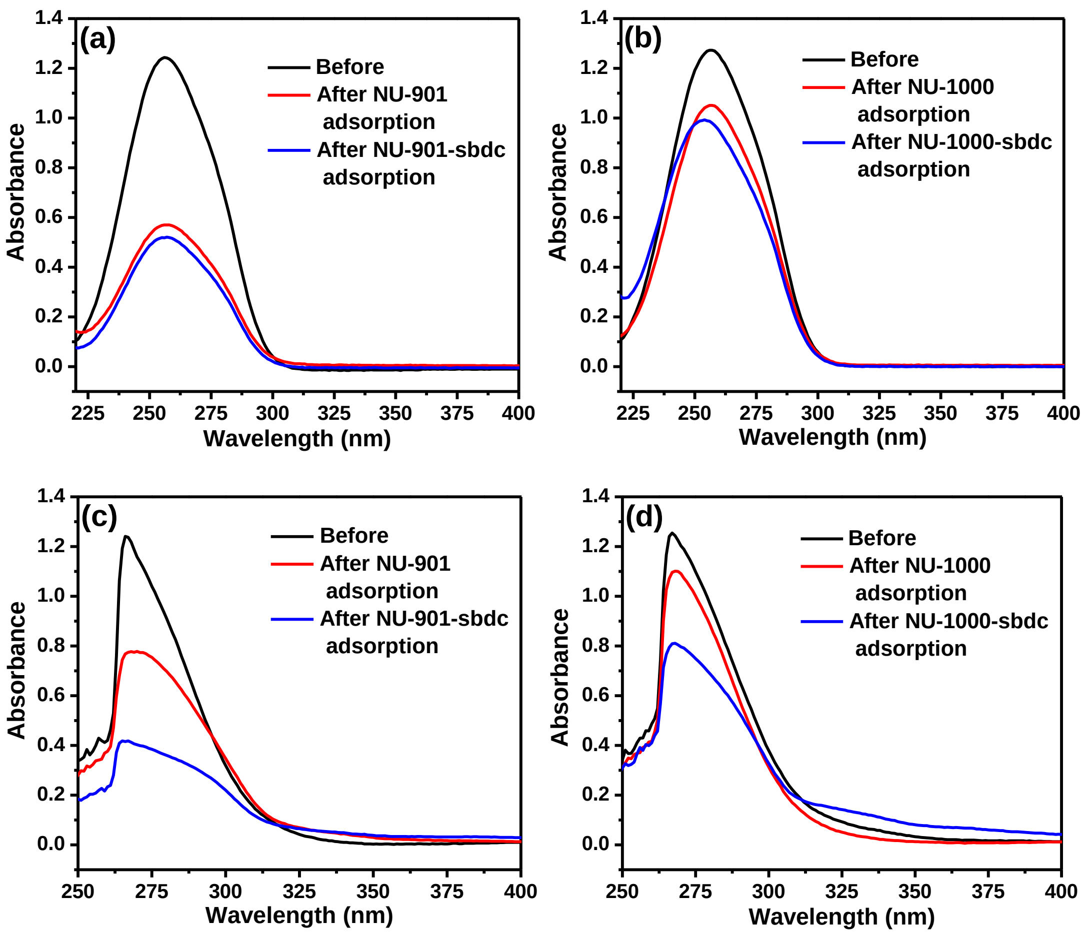

Fig. S4 Absorption spectra of the solutions of paraquat in water (a, b) and DMF (c, d) before and after the adsorption by NU-901 (a, c), NU-1000 (b, d) and their anionic derivatives.

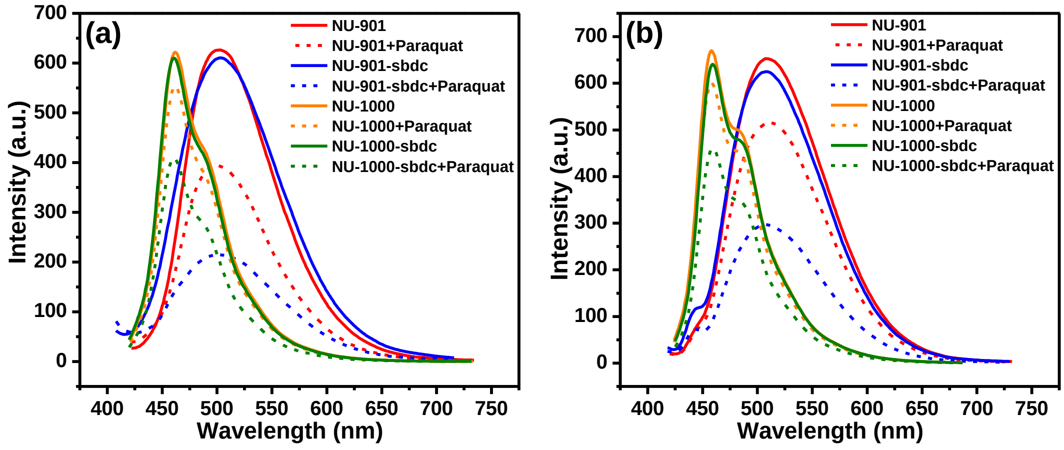

Fig. S5 Fluorescent spectra of NU-1000, NU-901, NU-1000-sbdc and NU-901-sbdc (0.01 g L^{-1}) before and after the addition of paraquat (1.0 μM) in (a) acetonitrile and (b) cyclohexane.

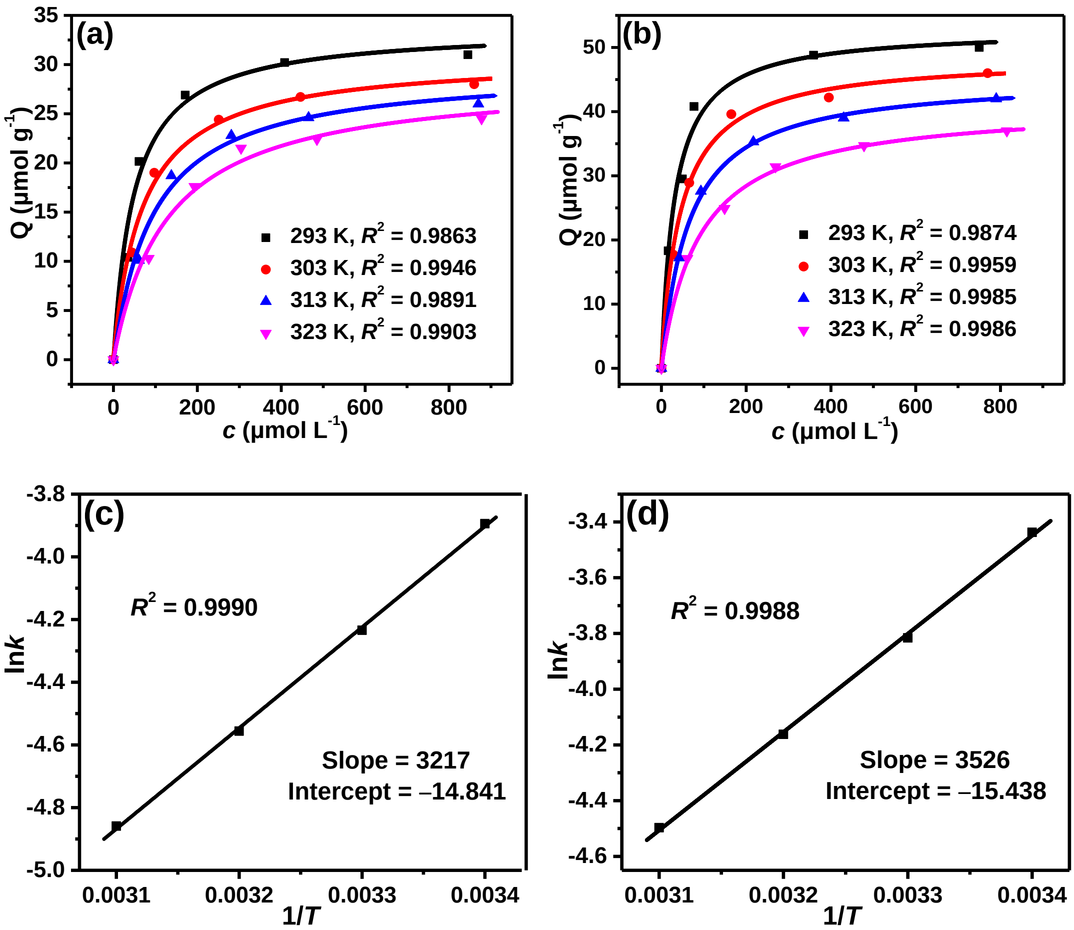

Fig. S6 Adsorption isotherms of paraquat on (a) NU-901 and (b) NU-901-sbdc in the medium of DMF. The thermodynamic fitting of the adsorption constants of (c) NU-901 and (d) NU-901-sbdc at different temperatures.

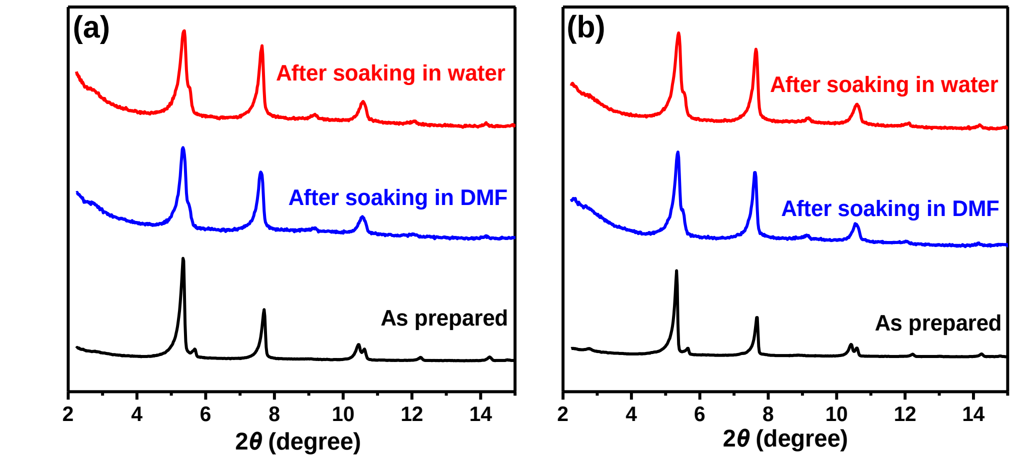

Fig. S7 PXRD patterns of (a) NU-901 and (b) NU-901-sbdc before and after the fluorescent detection of paraquat in water and DMF.

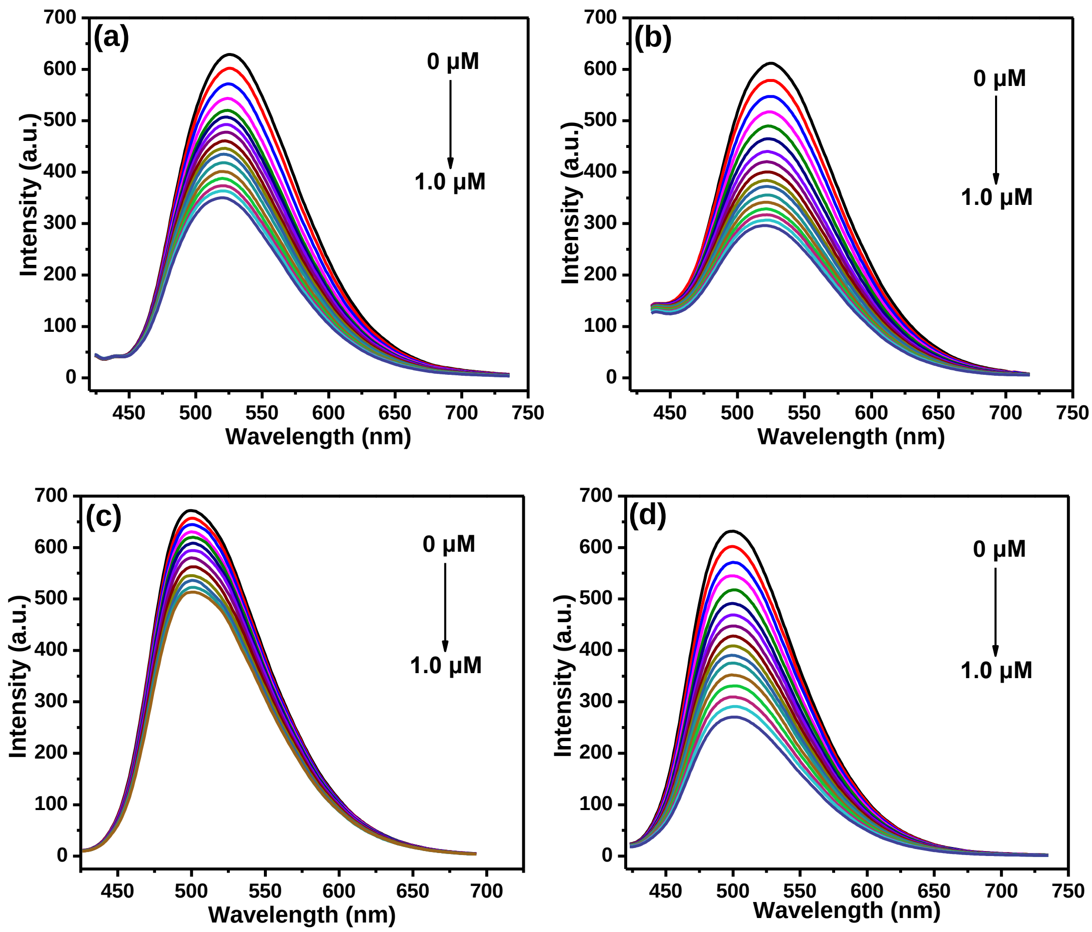

Fig. S8 Fluorescent spectra of NU-901 (a, c) and NU-901-sbdc (b, d) in the media of water (a, b) and DMF (c, d) after the addition of different concentrations of paraquat.

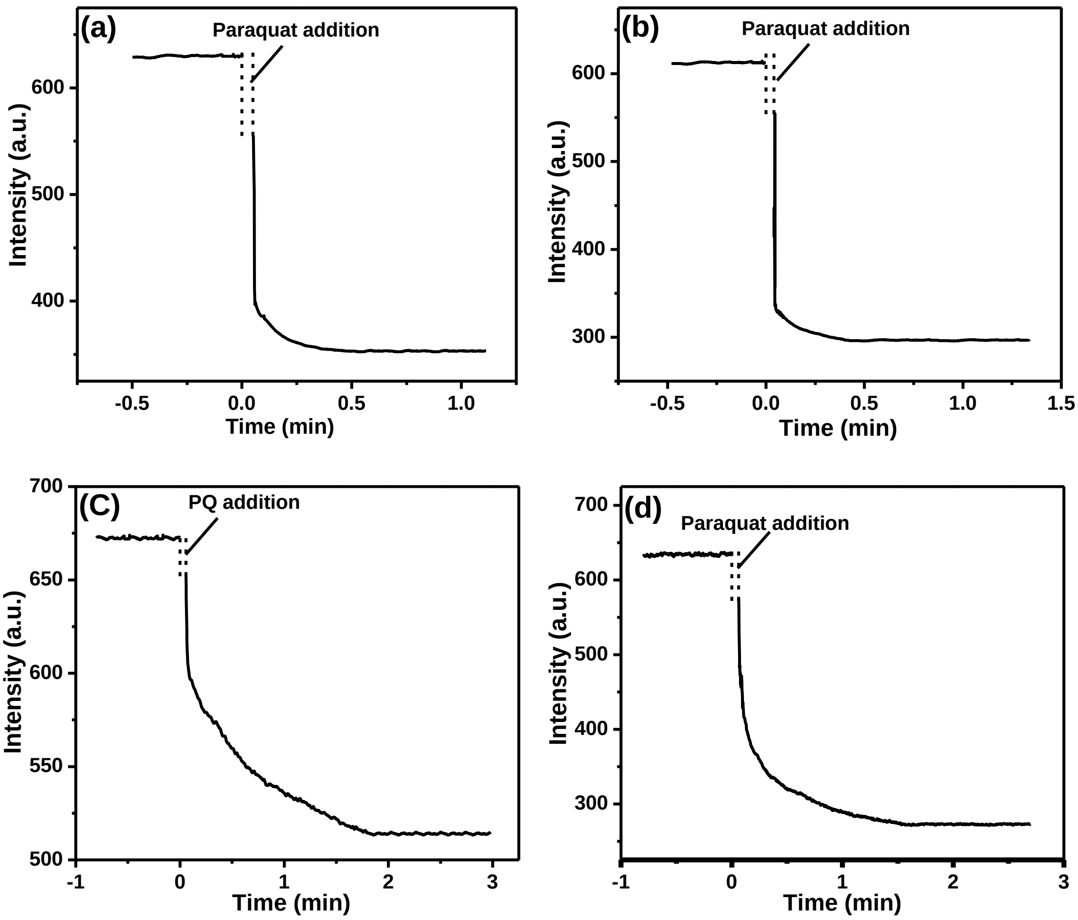

Fig. S9 Response time of NU-901 (a, c) and NU-901-sbdc (b, d) to paraquat (1.0 μM) in the media of water (a, b) and DMF (c, d).

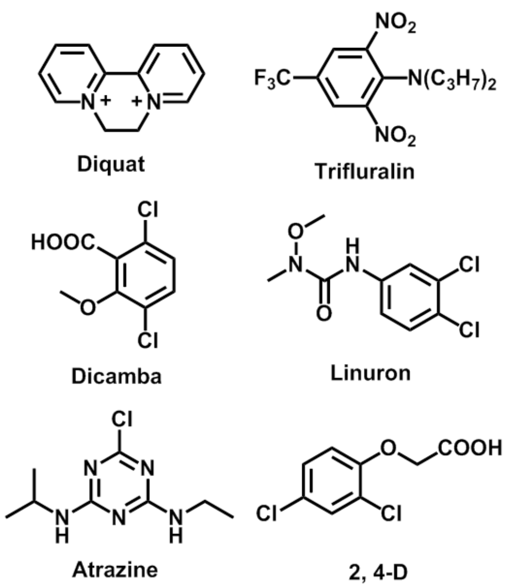

Fig.S10 Structures of the other agrochemicals.

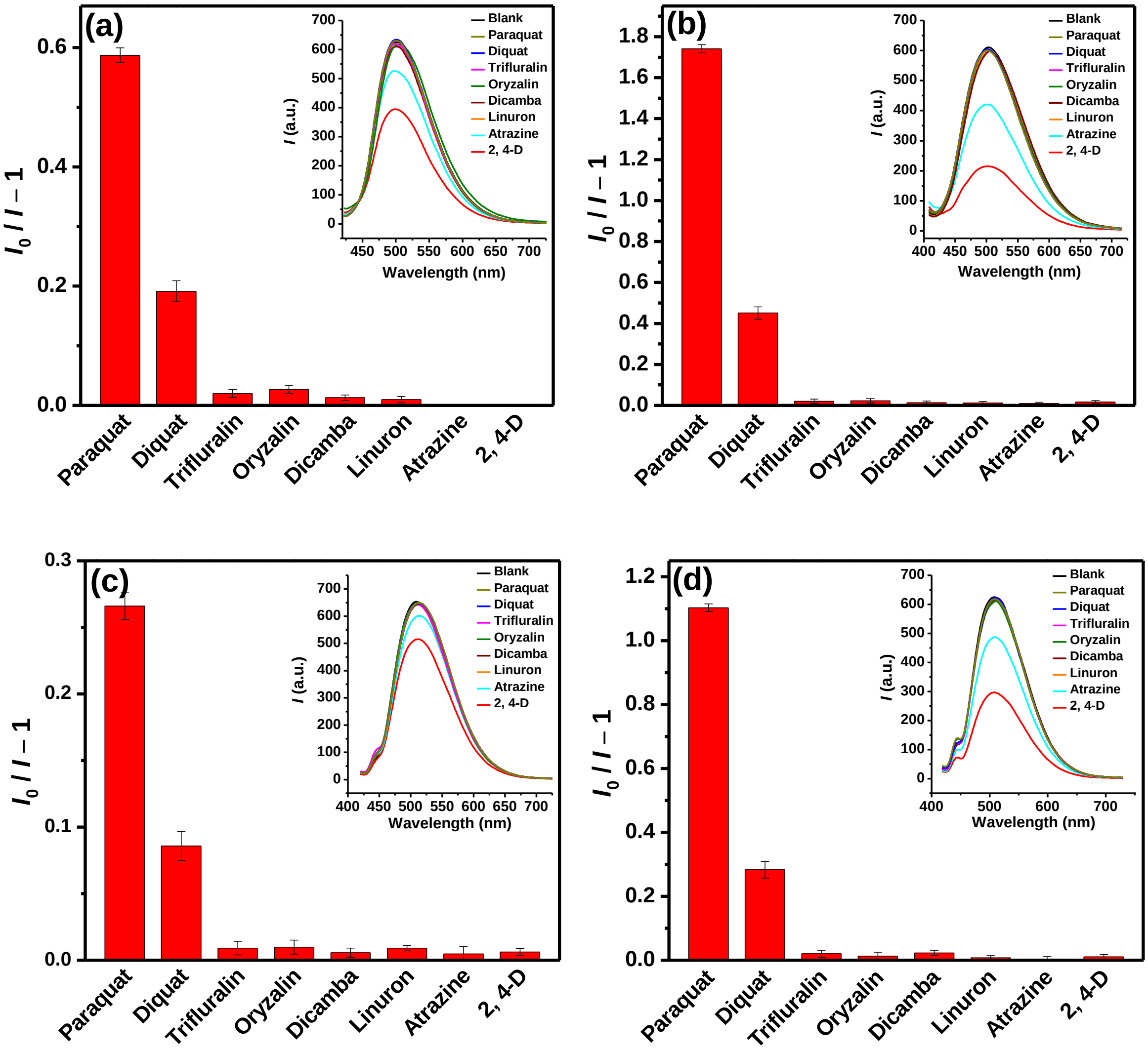

Fig.S11 Fluorescent responses of NU-901 (a, c) and NU-901-sbdc (b, d) (0.01 g L^{-1}) to different agrochemicals (1.0 μM) in acetonitrile (a, b) and cyclohexane (c, d).

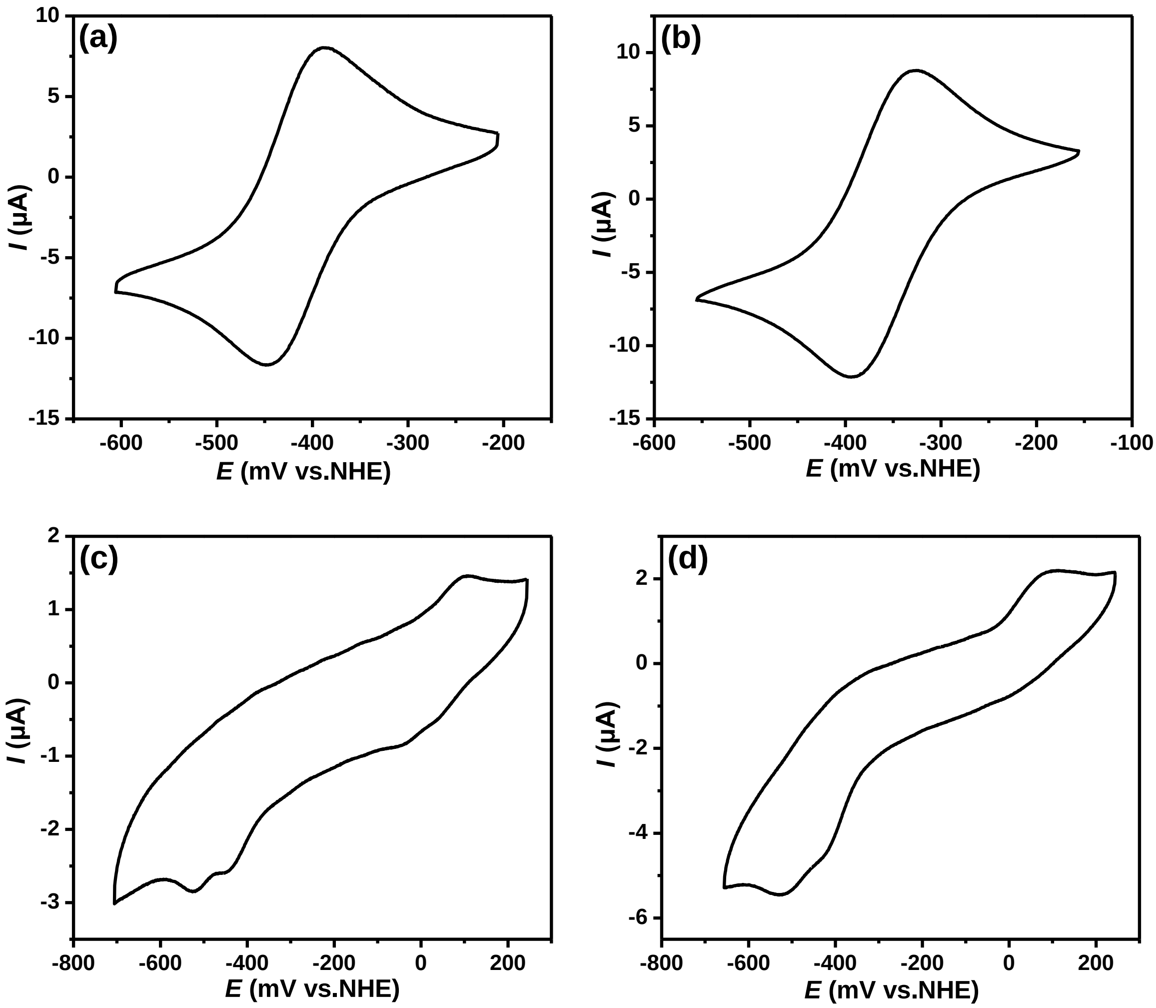

Fig. S12 Cyclic voltammetry curves of (a) paraquat, (b) diquat, (c) trifluralin and (d) oryzalin in water.

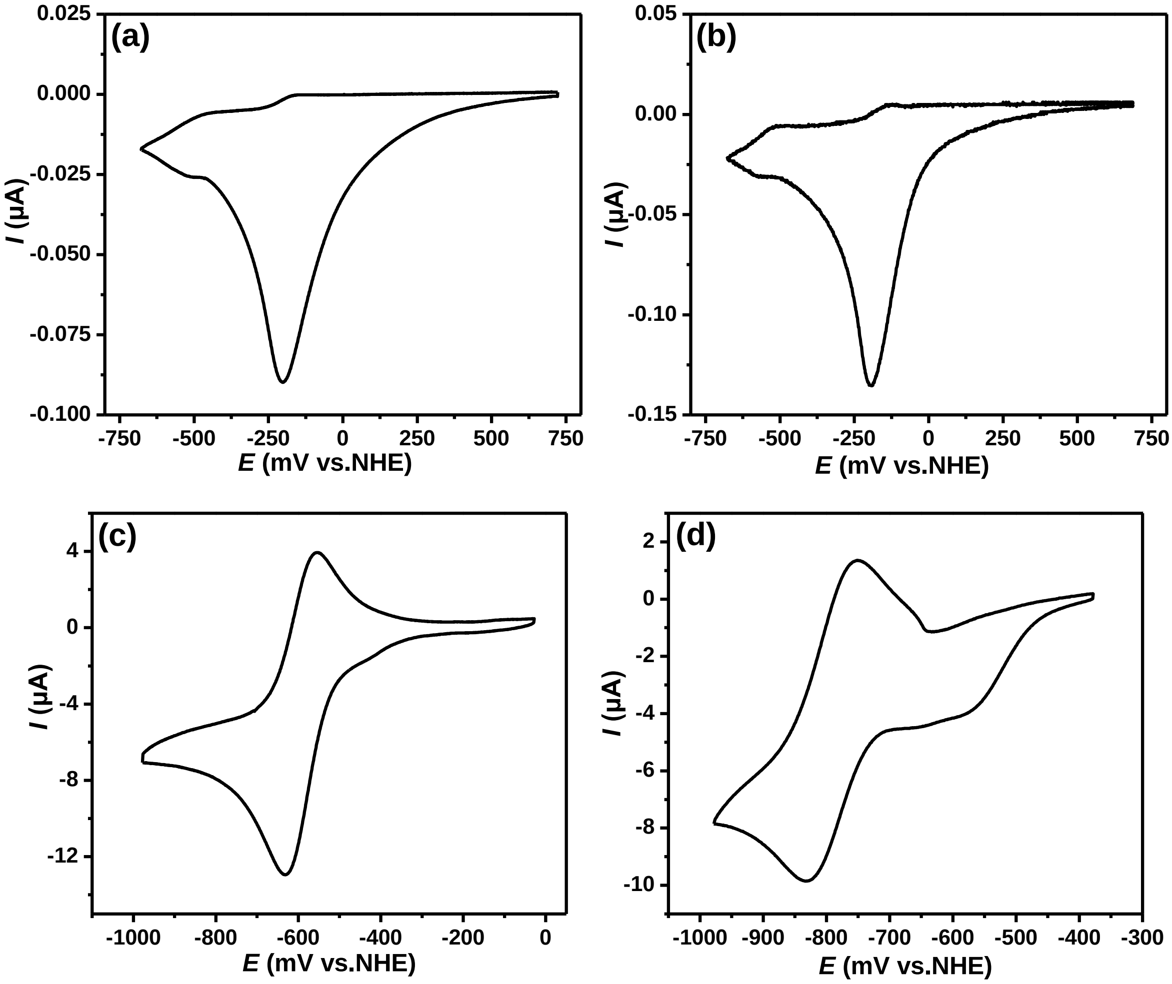

Fig. S13 Cyclic voltammetry curves of (a) paraquat, (b) diquat, (c) trifluralin and (d) oryzalin in DMF.

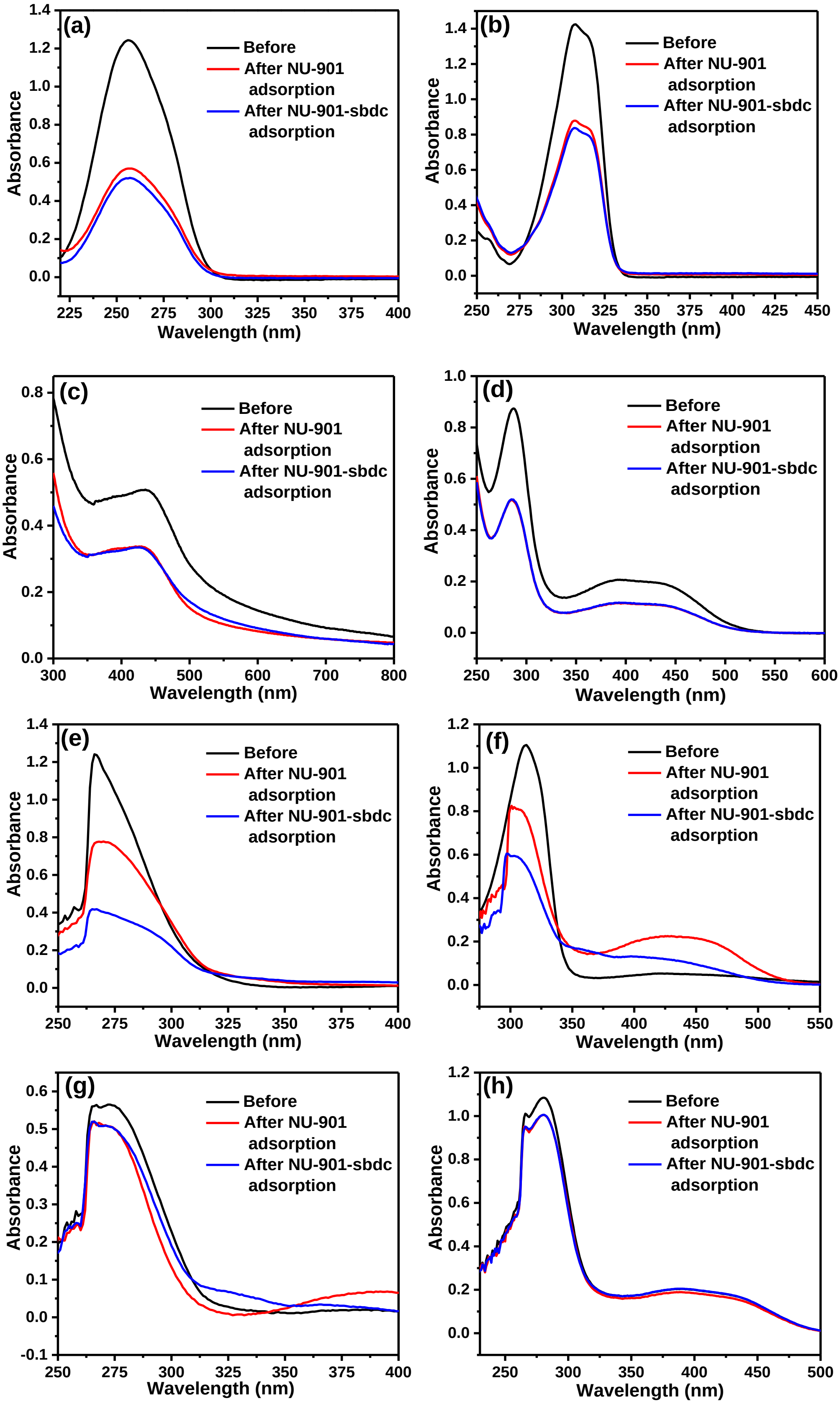

Fig. S14 Absorption spectra of the solutions of paraquat (a, e), diquat (b, f), trifluralin (c, g), and oryzalin (d, h), in water (a–d) and DMF (e–h) before and after the adsorption by NU-901 and NU-901-sbdc.

Table S1 Detection limits of recently reported paraquat responsive sensors.

Sensing material	Detection limit	Ref.
BN/MoS_2/Au nanoparticles	0.074 μM	1
tripodal tri-pillar[5]arene-based molecule	0.223 μM	2
pyrenyl nanoassembly	40 nM	3
N-GQDs/Hg^{2+}	73.9 nM	4
carboxymethyl-b-cyclodextrin supramolecule	10 μM	5
sod-type Tb-MOF	10 nM	6
$[Zn_2(cptpy)(btc)(H_2O)]_n$	9.73 μM	7
NU-901-sbdc (in DMF)	2.0 nM	This work
NU-901 (in DMF)	6.3 nM	
NU-901-sbdc (in H_2O)	2.0 nM	
NU-901 (in H_2O)	3.3 nM	

References

1. J. Zhang, Z. Lin, Y. Qin, Y. Li, X. Liu, Q. Li and H. Huang, *ACS omega*, 2019, **4**, 18398–18404.

2. Y.-F. Zhang, Z.-H. Wang, X.-Q. Yao, Y.-M. Zhang, T.-B. Wei, H. Yao and Q. Lin, Sens. *Actuators B: Chem.*, 2021, **327**, 128885.

3. H. Xu, K. Xiao, Q. Zhang, K. Huang, G. Song and Z. Yao, *ACS Sustain. Chem. Eng.*, 2020, **8**, 6861–6867.

4. F. Du, L. Sun, Q. Zen, W. Tan, Z. Cheng, G. Ruan and J. Li, *Sens. Actuators B: Chem.*, 2019, **288**, 96–103.

5. C. Liu, P. Wang, X. Liu, X. Yi, Z. Zhou and D. Liu, *New J. Chem.*, 2018, **42**, 17317–17322.

6. W. Du, Z. Zhu, Y. L. Bai, Z. Yang, S. Zhu, J. Xu, Z. Xie and J. Fang, *Chem. Commun.*, 2018, **54**, 5972–5975.

7. H. Chen, P. Fan, X. Tu, H. Min, X. Yu, X. Li, J. L. Zeng, S. Zhang and P. Cheng, *Chem. Asian. J.*, 2019, **14**, 3611–3619.